Effect of alloying additions on microstructure and properties of vertical-up MMA welds

1 — Method of theoretical assessment

Experimental results from research on microstructure and strength of vertical-up C-Mn MMA welds are theoretically assessed by **H K D H Bhadeshia** and **L-E Svensson,** who found that agreement between theory and experiment is remarkably good and present illustrative calculations covering a wide range of chemical compositions, *etc,* as a guide to weld design.

It has long been established that an understanding of variables which influence the microstructure of steel weld deposits is essential for optimum design of welding consumables and procedures. Procedures are in general developed empirically, with some assessment of mechanical properties. It is usually only in 'post mortems' that the macrostructure and microstructure are examined. This is not surprising in view of the complexity of microstructural phenomena although, ideally, the microstructure should take early prominence in any such research. To facilitate such work, bearing in mind the large number of variables involved, *e.g.* chemical composition, heat input and joint design, it is desirable to develop quantitative models relating variables to microstructure. Hence, considerable research has recently been devoted to use and development of phase transformations theory for prediction of steel weld microstructure.[1-5] It is possible to obtain reasonable quantitative estimates of the as-deposited (primary) microstructure of arc welds as a function of alloy chemistry (C, Si, Mn, Ni, Mo, Cr, V), welding process (submerged-arc and MMA), wide ranges of welding conditions and many other variables.[1-9] Note that trace elements such as oxygen, aluminium and titanium sometimes appear to have an influence on the microstructure of steel welds, but it has been demonstrated[1-9] that as long as the inclusion content is adequate for nucleation of acicular ferrite, it is possible to predict the variation of microstructure in a large number of arc welds on the basis of models discussed below and in Ref. 1-9.

Work aimed at obtaining general relationships between important mechanical properties and microstructure is as yet in its early stages, but it is already possible to estimate yield strength of the primary microstructure of arc welds.[10] The method has recently[11] been extended to enable prediction of yield and tensile strength of *multi-run* weld deposits to be made from a knowledge of independent solid solution strengthening data, strength of pure annealed iron and components due to microstructural strengthening. The mechanical property model also takes account of weld nitrogen concentration, since it has a detrimental effect on toughness.[12-15] A method based on the thermodynamics of nitrogen solution in liquid iron[16-19] has consequently been adapted to enable estimation to be made of nitrogen concentration as a function of chemistry, welding conditions and process.[11, 20]

Although the models mentioned above are approximate, and have yet to be tested and applied to other types of arc welding processes (or laser and electron beam welding), they are founded on phase transformations theory and should have wide applicability. The purpose of the present work is twofold. First, the models discussed above are for the first time tested against high quality data published recently[21] on the effect of alloying elements and heat input on *vertical-up* MMA welds. The model has been tested for welds deposited in the flat position only. The second purpose of this work arises from the fact that the models have now been reasonably established. Hence, they may be used for theoretical design of weld deposits without recourse to much experimental work. Many calculations have been carried out and results are presented in a form easy to assimilate.

METHOD OF ASSESSMENT

Primary microstructure prediction

Weld primary microstructure is that obtained during solidification and subsequent cooling to ambient temperature; it is also referred to as the as-deposited microstructure. It may subsequently be modified by post-weld heat treatment, or heat treatment arising from deposition of other layers in a multi-run weld, when the resulting structure is called the reheated or secondary microstructure.

Austenite grain structure

During solidification of arc welds grains of δ ferrite grow with columnar morphology, the direction of fastest growth lying roughly along that of maximum heat flow.[22] Austenite allotriomorphs eventually nucleate and grow along the δ-δ boundaries and, to a large extent, inherit the columnar morphology of the parent structure.[22, 23] The morphology of these grains can be approximated to in three dimensions by a series of long, space filling hexagonal prisms, cross sections of which have side length, a, with each prism extending a distance c along the solidification direction.[24] Since c is usually far greater than a,[24] it is the latter which features prominently in the theory for microstructural evolution in welds.[1] To measure accurately the parameter a requires considerable effort and so it is normally estimated by measuring $\bar{L}_m$, the mean linear intercept, measured on a transverse section, with the test lines aligned normally to the major dimensions of the columnar γ grains.[24] The following equation[24] is then used to obtain a:

$$\bar{L}_m \sim \pi a \cos(30°)/2 \qquad \ldots [1]$$

This equation is accurate if columnar grain major axes are aligned within the transverse section weld plane. This condition is approximately valid for welds deposited in the flat position, in which transverse sections always exhibit a highly anisotropic austenite grain structure.[24] On the other hand, there is some experimental evidence that for vertical-up welding the austenite grain morphology observed on transverse sections is less anisotropic, often tending towards an equiaxed structure.[25, 26] The c axes of the hexagonal prisms are thus inclined at a relatively shallow angle (estimated to be 66° by Evans[25]) to the welding direction, and thus to the plate surface.

Austenite grain size is crucial in determining the type of microstructure which evolves on cooling.[1, 5, 27] There exist crude methods for estimating the necessary γ grain parameters for welds deposited in the flat position[3] but there is as yet no similar procedure for vertical-up welds. Fortunately, for the welds assessed in the present study,[21, 28, 29] Court and Pollard[21] have reported *random* linear intercept measurements done on transverse sections (henceforth referred to as $\bar{L}_t$). If it is assumed that the γ grain c axes are aligned at 66° to the welding direction[25] and that a side of the hexagonal cross section is

Harshad Bhadeshia, BSc, MSc, CEng, is a lecturer in the Department of Materials Science and Metallurgy, University of Cambridge, and Lars-Erik Svensson is Research Manager at ESAB AB, Gothenburg.

aligned to the surface, then it follows that for grains observed on a transverse section of the weld

$$P = a + 2[(a^2/4) + \beta^2 a^2]^{0.5} \quad \ldots [2]$$

where P is the perimeter *per* grain (taking account of the sharing of edges between adjacent grains) and $\beta = 2\cos(30°)/\cos(66°)$. The area per grain is given by

$$A = 3\beta a^2. \quad \ldots [3]$$

The amount of boundary line per unit area of the plane of section is thus given by:[30, 31]

$$L_A = P/A \quad \ldots [4]$$

so that

$$L_A = \{1 + 2(0.25 + \beta^2)^{0.5}\}/(3\beta a) \quad \ldots [5]$$

Since $\bar{L}_t = \pi/(2L_A)$,[30, 31] it follows that

$$\bar{L}_t = 1.372\ \bar{L}_m \quad \ldots [6]$$

In fact, the angle of 66° given by Evans[25] may be subject to many experimental variables; in the authors' experience, and from micrographs presented by Court and Pollard,[21] the angle is likely to be shallower, with more or less equiaxed austenite grains appearing in transverse section. As the angle becomes more shallow, $\bar{L}_t$ tends to $\bar{L}_m$. Consequently, as will become apparent later, we have carried out microstructure calculations for the limits $\bar{L}_t = 1.372\bar{L}_m$ and $\bar{L}_t = \bar{L}_m$.

Cooling conditions

Weld microstructure develops anisothermally during cooling to ambient temperature. To calculate microstructure development during cooling it is necessary to describe the cooling curve of the fusion zone in an analytical manner.[1, 3] The cooling rate ($\partial T/\partial t$) in the fusion zone, for the temperature range 800-500°C, is expressed as a function of temperature (T) by an equation of the form:[3]

$$\partial T/\partial t = \{C_1(T-T_i)^{C_2}\}/\{Q\eta\} \quad \ldots [7]$$

where t represents time, T_i the interpass temperature or preheat, Q the nominal electrical energy input per unit length of weld deposited (J/m) and η the arc transfer efficiency (assumed to be 0.775 for MMA welds, this being a mean of typical values[32]). C_1 and C_2 are empirical constants derived by fitting experimental cooling curves to the above equation, and have values of approximately 1325 and 1.6, respectively,[3] for MMA welds deposited in the flat position, joint design corresponding to ISO-2560-1973. Such data do not exist for vertical-up welds. However, Evans[25] has reported the time taken for such welds to cool from 800-500°C; values of $C_1 = 1125$ and $C_2 = 1.7$ were found to represent the cooling time of 22sec (800-500°C) that he reported for vertical-up welds with 3.4 kJ/mm heat input. It should be noted that since the full cooling curves have not been reported, values of these constants cannot be derived uniquely since the form of the T-t curve may vary between 800-500°C. However, the values chosen are close to those of the MMA welds produced in the flat position. It is also relevant that joint design and welding procedure studied by Evans differ in detail from procedures relevant to Court and Pollard's work, but since the results all refer to multi-run welds with three dimensional heat flow, the difference may be acceptably small as far as cooling conditions are concerned.

Values of the constants C_1 and C_2 as deduced above, together with [7], are used to represent the cooling conditions of vertical-up welds in the microstructural calculations which follow (Fig. 1).

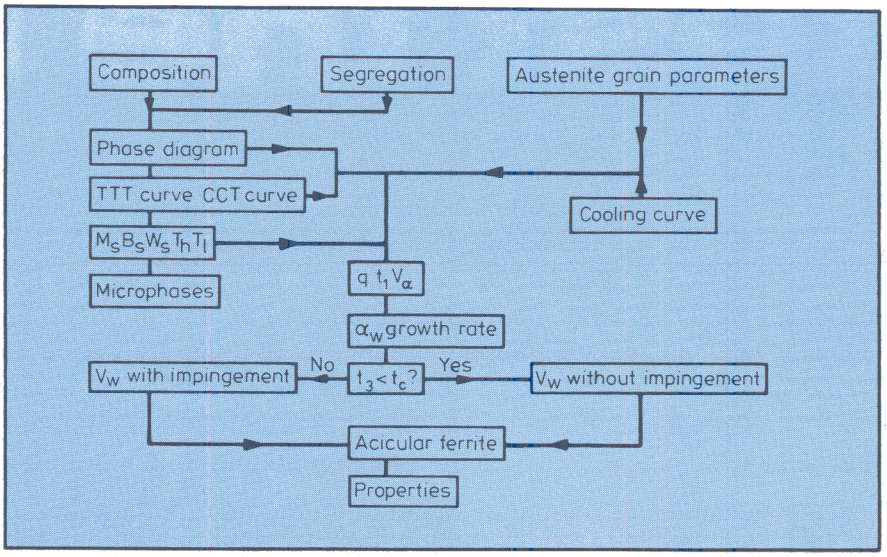

△

1 Steps involved in calculation of primary microstructure.

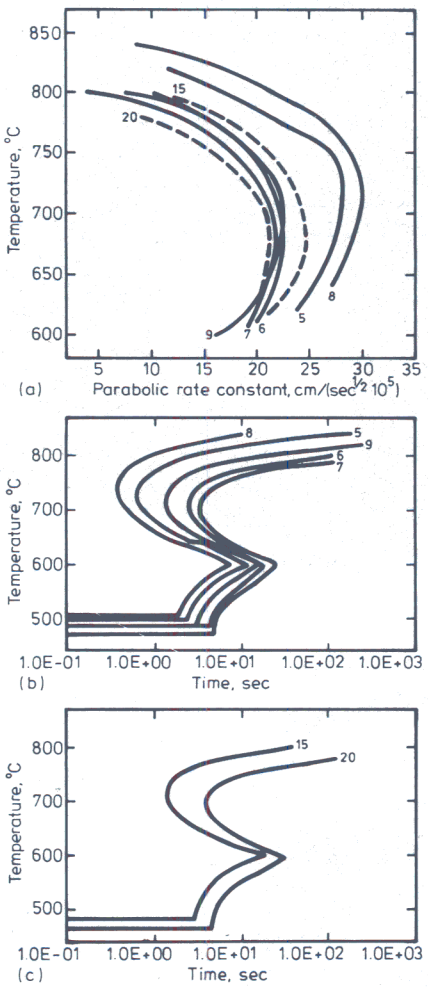

2 Calculated: *a)* One dimensional parabolic thickening rate constants for alloys W5-W20 as function of transformation temperature; *b)* TTT diagrams for reaction initiation in alloys W5-W9; *c)* TTT diagrams for reaction initiation in alloys W15, W20.

Primary microstructure calculation

Detailed discussions of transformation mechanisms can be found in some recent reviews.[33-36] Here the method is outlined (Fig. 1) by which the microstructure is calculated, and the nature of the microstructural constituents summarised. Experimental data analysed are from the work of Court and Pollard; essential details of those experiments are presented in Table 1.

Allotriomorphic ferrite (α) is the first phase to form during cooling of austenite in low alloy steels. It nucleates at the austenite grain boundaries and grows by a diffusional transformation mechanism which involves, at least, reconstructive diffusion,[33] which is the diffusion necessary to achieve the lattice change with minimum strain. Growth of α is anisotropic, the rate being highest along the γ boundaries which soon become decorated with layers of α. Thickness of these layers can be estimated as a function of time, temperature and alloy chemistry by assuming one dimensional, paraequilibrium, carbon diffusion-controlled growth*. For isothermal transformation,[37] the half thickness q of the ferrite layers varies as

$$q = \alpha_1 t^{0.5} \quad \ldots [8]$$

where α_1 is the one-dimensional parabolic thickening rate constant (Fig. 2) and t is the time at temperature.* The parabolic

* *The theory for ferrite growth in iron and its alloys has been reviewed by Bhadeshia.[33] This should be consulted for detailed information on phase transformation.*

rate constant is determined by solving the Zener/Dubè equation (equation 5.13a of Ref. 33)

$$\Omega=(0.25\pi/\bar{D})^{0.5}\alpha_1 [\mathrm{erfc}(0.5\alpha_1/(\bar{D})^{0.5})] \exp\{(\alpha_1)^2/(4\bar{D})\} \quad \ldots [9]$$

where Ω is a dimensionless supersaturation given by

$$\Omega=(x^{\gamma\alpha}-\bar{x})/(x^{\gamma\alpha}-x^{\alpha\gamma}) \quad \ldots [10]$$

and $x^{\gamma\alpha}$ and $x^{\alpha\gamma}$ are the paraequilibrium carbon concentrations in austenite and ferrite, respectively, obtained from the calculated phase diagrams, and $\bar{x}$ is the average carbon concentration in the alloy.

The diffusion coefficient (D) of carbon (x) in austenite is known to be strongly concentration dependent and this causes complications in kinetic analysis of diffusion-controlled reactions in steels. However, it has been demonstrated by Trivedi and Pound[38] a weighted average diffusivity $\bar{D}$ can be used instead, where $\bar{D}$ is defined as

$$\bar{D}=\int_{x_1}^{\bar{x}} D\{x,T\}\,dx/(\bar{x}-x_1) \quad \ldots [11]$$

where x_1 is the carbon concentration in austenite at the interface, in this instance equal to $x^{\gamma\alpha}$. The weighted average diffusivity is valid only for steady state growth, but it has been shown[6] using numerical analysis that it is a good approximation for allotriomorphic ferrite growth in steel welds.

Welding is anisothermal, so that the thickness of the α has to be determined by integration over the time t=0 to t=t_1, during which it grows[1]

$$q=\int_{t=0}^{t_1} 0.5\alpha_1 t^{-0.5}\,dt \quad \ldots [12]$$

where time *t* is zero at a temperature T_H when the growth of α begins. The time t_1 corresponds to temperature T_L, at which α growth ceases and gives way to formation of Widmanstätten ferrite. T_H is calculated with the help of a computed time-temperature-transformation curve (TTT)[37] using the Scheil method[38] and treating the continuous cooling curve (CCT) as a combination of many successive isothermal transformations from the cooling curve (in effect, by converting the TTT curve into a continuous cooling transformation curve). The calculated TTT diagrams are presented in Fig. 2. The kinetic calculations also require a knowledge of the paraequilibrium phase diagram to fix the compositions of the phases at the transformation interface (Fig. 3); the paraequilibrium phase boundaries are calculated as in Ref. 39.

As the transformation temperature decreases, diffusion becomes sluggish and gives way to *displacive* transformations, which are kinetically (though not thermodynamically) favoured. The temperature T_L at which this transition occurs is approximated by the point at which the diffusional and displacive C curves of the TTT diagrams cross. At temperature T_L, the growth of allotriomorphic ferrite is complete, and the calculated thickness of the layers of α can be converted into a volume fraction V_α with the help of the austenite grain size[1]

$$V_\alpha = 2.04[4qC_3(a-qC_3)/a^2]+0.035 \quad \ldots [13]$$

where C_3=tan{30°} and *a* is the austenite grain size as discussed earlier.

Displacive transformations do not involve any reconstructive diffusion so that substitutional or iron atoms do not diffuse during reaction.[33] Consequently, the transformations are accompanied by macroscopic displacements reflecting the co-ordinated movement of atoms during the lattice change, the displacements having the characteristics of invariant plane strains. Their morphology is thus dominated by the need to minimise strain energy and the strain energy terms must be taken into account during kinetic and thermodynamic calculations. Plates of Widmanstätten ferrite (α_W) grow at relatively low undercoolings by a displacive paraequilibrium mechanism which involves simultaneous growth of pairs of mutually accommodating plates of ferrite, so that the strain energy of transformation is reduced.[36, 40] Widmanstätten ferrite and bainite (α_b) both nucleate by the same mechanism and are both represented, at least initially, by the same C curve on the time temperature transformation (TTT) diagram. Bainite, which develops in the form of sheaves of small platelets, can only grow at a higher undercooling because it deviates further from equilibrium, forming by diffusionless transformation from austenite (the carbon redistributing into γ subsequent to transformation), the strain energy term also being higher since the plates do not form in an accommodating manner.[36] Because of the large austenite grain size and low alloy content of most steel weld deposits, grain boundary nucleated bainite is not found in significant quantities in weld deposits.

Lenticular plates of acicular ferrite (α_a) form by the same transformation mechanism as bainite, but have different morphology because nucleation occurs intragranularly at inclusions (rather than at γ grain boundaries) and development of sheaves is stifled by hard impingement between plates nucleated at neighbouring sites.[41, 42] Nucleation of acicular ferrite plates can also occur sympathetically,[43] so that a one to one correspondence with inclusions is not expected. The exact mechanism of sympathetic nucleation of acicular ferrite is not established, but in the present context, the term implies that formation of an initial plate of acicular ferrite stimulates nucleation of other plates in its vicinity. The stimulation may arise because new plates[44] tend to form in a manner which compensates the invariant plane strain shape change that accompanies growth of the initial plate acicular ferrite,[42] but this is as yet speculation.†

The growth rate of Widmanstätten ferrite at temperature T_L, can for typical weld deposits be shown to be so high that the transformation is virtually isothermal†. The theory necessary for calculation of Widmanstätten ferrite growth rate is involved, but the subject has recently been assessed and reviewed in detail;[45] the interested reader can find the method and information necessary for such calculations in that paper. While the growth rate of Widmanstätten ferrite, *i.e.* G_w, is an important factor in determining the evolution of microstructure in weld deposits, the volume fraction of Widmanstätten ferrite does not correlate with G_w. Acicular ferrite which forms immediately afterwards complicates the problem since it nucleates intragranularly; it can therefore interfere with the growth of Widmanstätten ferrite, and impingement between these phases must be taken into account†. The welds studied by Court and Pollard contain a significant amount of alloying additions (which reduce G_w) and, in all instances, calculations (Table 2) predicted that growth of Widmanstätten ferrite is limited by impingement with intragranularly nucleated acicular ferrite,

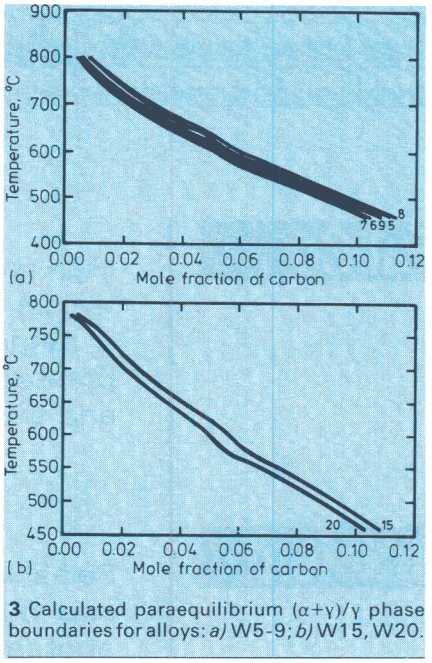

3 Calculated paraequilibrium (α+γ)/γ phase boundaries for alloys: *a)* W5-9; *b)* W15, W20.

† *Ref. 43 also suggests that acicular ferrite should be regarded as intragranularly nucleated Widmanstätten ferrite. However, the evidence presented is ambiguous. For example, observation of 'steps' at the transformation interface was taken to support the suggestion; however, this simply represents a mechanism of interface motion and not a mechanism of transformation. Even martensite may grow by a step mechanism. Enrichment of austenite in carbon, as a consequence of formation of acicular ferrite was also interpreted to imply that the reaction involves partitioning of carbon during transformation. However, partitioning could occur after transformation, and there is strong thermodynamic evidence[41, 42] that acicular ferrite grows by diffusionless transformation, with subsequent rejection of carbon into the residual austenite. The evidence all shows that acicular ferrite is in fact intragranularly nucleated bainite; indeed, if the density of intragranular sites is reduced, the microstructure is found to change from acicular ferrite to conventional bainite.*[41, 44]

Table 1 Chemical composition, wt %, except for N and O, ppm, and grain size, for vertical-up welds

Weld	C	Si	Mn	N	O	Grain size, L_t, μm
W8	0.06	0.74	0.92	88	272	130
W5	0.06	0.72	1.15	110	250	140
W9	0.07	0.66	1.40	112	295	170
W6	0.06	0.76	1.70	90	230	185
W7	0.06	0.71	1.81	89	271	190
W15	0.06	0.32	1.38	110	360	170
W20	0.06	0.35	1.81	130	330	190

Table 2 Calculated data for welds W5-20

Weld	Ae3', °C	G_w, μm/sec	q, μm	T_H-T_L, °C	V_P
W8	853	141	9.0	792-611	0.16
W5	821	142	8.3	773-610	0.28
W9	812	80	7.0	747-609	0.31
W6	794	91	7.1	721-609	0.37
W7	791	80	6.7	704-609	0.39
W15	800	107	8.4	753-610	0.35
W20	786	78	7.1	712-609	0.40

so that the α_W plates are unable to grow right across the γ grains. This is consistent with micrographs presented in Ref. 21.

Formation of α, α_a and α_W usually consumes most of the austenite and the remainder is either retained or decomposes to martensite or degenerate pearlite; these products are collectively called microphases in welding terminology, and since the volume fraction involved is normally small, they are implicitly included in α_a. It follows that the sum of the volume fractions V_α, V_w and V_a (of α, α_W and α_a respectively) is unity, so that V_a can be calculated from a knowledge of just V_α and V_w. The full procedure is summarised in Fig. 1.

Secondary microstructure calculation

In multi-run welds metal deposited first is influenced significantly by additional thermal cycles during deposition of subsequent layers. Some regions of the original structure are thus reheated to temperatures high enough to cause complete reverse transformation into austenite which, during cooling, retransforms into a variety of transformation products. Other regions may simply be tempered by deposition of subsequent runs. The microstructure of reheated regions is called *secondary microstructure.* There is no satisfactory model to predict this microstructure, in the detail discussed above for primary regions, although detailed long term research is in progress.

On the other hand, for modelling weld deposit strength, Svensson *et al*[11] show that it is possible to make some crude assumptions for multi-run welds; a volume fraction V_p is defined to include primary microstructure and reheated regions which are *fully* reaustenitised, on the grounds that these regions are mechanically similar to the as-deposited regions. The remainder V_s=1-V_p includes all regions which have been tempered or partially reaustenitised and lost most of the microstructural component of strengthening. V_p can be estimated from the alloy chemistry since this in turn influences the extent of the austenite phase field via the Ae3' temperature (Table 2). Details are given in Ref. 11. Finally, it should be emphasised again that the volume fractions V_p and V_s *do not* refer to the volume fractions of primary and secondary microstructures, respectively, but are defined in a peculiar way to simplify the task of estimating multi-run weld strength; thus, V_p includes the primary microstructure and regions which are fully reaustenitised due to deposition of further material, and V_s includes all other regions which have essentially lost most of the microstructural component of strength.[11]

References

1 Bhadeshia H K D H, Svensson L-E and Gretoft B: 'A model for the development of microstructure in low alloy steel welds'. *Acta Metallurgica* 1985 **33** 1271-1283.

2 Gretoft B, Bhadeshia H K D H and Svensson L-E: 'Development of microstructure in the fusion zone of steel weld deposits'. *Acta Stereologica* 1986 **5** 365-371.

3 Svensson L-E, Gretoft B and Bhadeshia H K D H: 'An analysis of cooling curves from the fusion zone of steel weld deposits'. *Scand J Metall* 1986 **15** 97-103.

4 Bhadeshia H K D H, Svensson L-E and Gretoft B: 'Prediction of the microstructure of the fusion zone of multicomponent steel weld deposits'. Proc conf: 'Advances in welding science and technology'. 1987 225-229, ASM, Metals Park, Ohio, USA.

6 Bhadeshia H K D H, Svensson L-E and Gretoft B: 'Prediction of the microstructure of submerged-arc linepipe welds'. Proc conf: 'Welding and performance of pipelines–III'. 1986, The Welding Institute, Cambridge, UK.

7 Svensson L-E, Gretoft B and Bhadeshia H K D H: 'Computer-aided design of electrodes for manual metal arc welding'. Proc 1st int conf 'Computer technology in welding'. 1986, The Welding Institute, Cambridge, UK.

8 Svensson L-E and Bhadeshia H K D H: 'The design of submerged-arc weld deposits for high-strength steel welds'. Proc IIW conf, Vienna, 1988.

9 Bhadeshia H K D H, Svensson L-E and Gretoft B: 'An analysis of the primary microstructure of Cr and Mo containing low alloy steel welds'. Proc 4th Scand symp on Mat Sci, 1986, 153-158, Norwegian Institute of Technology, Norway.

10 Sugden A A B and Bhadeshia H K D H: 'A model for the strength of the as-deposited regions of steel welds'. Metall Trans A 1988 **19A** (June).

11 Svensson L-E, Gretoft B, Sugden A A B and Bhadeshia H K D H: 'Computer-aided design of electrodes for arc welding, Part II'. Proc 2nd int conf 'Computer technology in welding' 1988, The Welding Institute, Cambridge, UK.

12 Lancaster J F: 'Metallurgy of welding'. 1988. Publ Allen and Unwin, London.

13 Keown S R, Smaill J S and Erasmus L A, *Metals Technology* 1976 **3** (194).

14 Judson P and McKeown D: 'Advances in the control of weld metal toughness'. 2nd int conf 'Offshore welded structures'. 1982, The Welding Institute, Cambridge, UK.

15 Oldland R B: 'Al and N effects on the microstructure and properties of single pass SMA welds'. *Australian Welding Research* 1985 (Dec) 31.

16 Pehlke R D and Eliott J F, *Trans AIME* 1960 **218** 1088.

17 Evans D B and Pehlke R D, *Trans AIME* 1965 **233** 1620.

18 Wagner C: 'Thermodynamics of alloys'. Publ Addison-Wesley, 1952, Cambridge, Massachusetts, USA.

19 Kobayashi T, Kuwana T and Kiguchi R, *J Jap Weld Soc* 1972 **41** 308.

20 Bhadeshia H K D H, Svensson L-E and Gretoft B: 'Nitrogen in submerged-arc weld deposits'. *J Mat Sci* 1988.

21 Court S and Pollard G: 'The effects of Mn and Si on the microstructure and properties of SMA steel weld deposits'. Proc conf 'Welding metallurgy of structural steels'. 1987, *TMS-AIME,* Pennsylvania, USA.

22 Davies G J and Garland J G: 'Solidification of welds'. *Int Metall Rev* 1975 **20** 83.

23 Widgery D J and Saunders G G: 'Microstructures in steel weld metals'. *Welding Institute Research Bulletin* 1975 **16** (10) 277-281.

24 Bhadeshia H K D H, Svensson L-E and Gretoft B: 'The austenite grain structure of low alloy steel weld deposits'. *J Mat Sci* 1986 **21** 3947-3951.

25 Evans G M: 'Effect of welding position on the microstructure and properties of C-Mn all-weld metal deposits'. IIW Doc IIA-529-81.

26 Svensson L-E: 'The effect of alloy chemistry on arc welds'. ESAB internal report on vertical-up welds, 1986 (Mar).

27 Fleck N A, Grong O, Edwards G R and Matlock D K: 'Role of filler metal wire and flux composition in submerged-arc weld metals'. *AWJ* res supp, 1986 (May) 113s.

28 Abson D J: 'The influence of manganese and preheat on the microstructure and mechanical properties of vertical-up MMA welds in 38mm thick C-Mn-Nb steel plate, part 1'. Welding Institute Members Report 194/1982.

29 Abson D J: 'The influence of manganese and coating basicity on the microstructure and mechanical properties of vertical-up MMA welds in 38mm thick C-Mn-Nb steel plates, final report'. Welding Institute Members Report 309/1986.

30 Dehoff R T: 'Quantitative microscopy'. 1968, McGraw Hill, New York, USA.

31 Underwood E E: 'Quantitative stereology'. 1970, Addison-Wesley, Reading, Massachusetts, USA.

32 Easterling K: 'Introduction to the physical metallurgy of welding'. Publ 1982, Butterworths, London, and Cochrane R C: IIW Doc IX-1248-82.

33 Bhadeshia H K D H: 'The diffusional formation of ferrite in iron and its alloys'. *Progress in Materials Science* 1985 **29** 321-386.

34 Abson D J and Pargeter R J: 'Factors influencing the as-deposited strength, microstructure and toughness of MMA welds suitable for C-Mn steel fabrications'. *Int Met Rev* 1986 **31** 141-194.

35 Grong O and Matlock D K: 'Microstructural development in steel weld metals'. *Int Met Rev* 1986 **31** 27-48.

36 Bhadeshia H K D H: 'Review on the bainite transformation in steels'. Proc conf 'Phase transformations '87'. Institute of Metals.

37 Bhadeshia H K D H: 'A thermodynamic analysis of isothermal transformation diagrams'. *Metal Science* 1982 **16** 159-165.

38 Christian J W: 'Theory of transformations in metals and alloys'. 2nd ed Part I 1975 Pergamon Press, Oxford, UK.

39 Bhadeshia H K D H and Edmonds D V: 'The mechanism of the bainite transformation in steels'. *Acta Metallurgica* 1980 **28** 1265-1273.

40 Bhadeshia H K D H: 'A rationalisation of shear transformations in steels', *Acta Metallurgica* 1981 **29** 1117-1130.

41 Yang J R and Bhadeshia H K D H: 'Thermodynamics of the acicular ferrite transformation in alloy steel welds'. Proc conf 'Advances in welding science and technology'. 1987, ASM, Metals Park, Ohio, 187-191.

42 Strangwood M S and Bhadeshia H K D H: 'Mechanism of the acicular ferrite transformation in steel welds deposits'. Proc conf 'Advances in welding science and technology'. 1987, ASM, Metals Park, Ohio, 209-213.

43 Ricks R A, Howell P R and Barritte G S: 'The nature of acicular ferrite in HSLA steel weld deposits'. *J Mat Sci* 1982 **17** 732.

44 Yang J R and Bhadeshia H K D H: 'Reaustenitisation in steel weld deposits'. Welding metallurgy of structural steels. *TMS-AIME* 1987 495-504.

45 Bhadeshia H K D H: 'Diffusion-controlled growth of ferrite plates in plain carbon steels'. *Materials Science and Technology* 1985 **1** 497-504.

46 Daigne J, Guttman M and Naylor J P: 'Influence of lath boundaries and carbide distribution on the yield strength of 0.4% C tempered martensitic steels'. *Materials Science and Engineering* 1982 **56** 1-10.